Paper-derived bioactive ceramics for complex shape bone implants

H. Lorenz, A. Bonet, A. Ayrikyan, P. Greil, and N. Travitzky*

Department of Materials Science and Engineering (Glass and Ceramics), University of Erlangen-Nuremberg, Erlangen, Germany

This paper reports the preparation and properties of paper-derived bioactive ceramic materials that allow easy fabrication of complex-shape implants for bone replacement and regeneration. Tricalcium phosphate (β-TCP), hydroxyapatite (HAP) and bioactive glass (BaG) were used as filler materials in the feedstock for the manufacturing of porous ceramic sheets by a novel preceramic paper processing method. The preceramic papers were sintered at temperatures ranging from 630 to 1250°C, depending on the filler material. The initial preceramic papers and the obtained ceramics were characterized in terms of microstructure and composition, and their porosity and density were measured and compared. The mechanical strength of the sintered specimens was measured using the ball-on-three-ball test and the three point bending test. The open porosity of the as-fabricated paper-derived biomaterials was in the range of 37–64%, their strength varied between approximately 7.6 and 33.1 MPa, while their Young's modulus ranged between 0.33 and 1.53 GPa.

Keywords: paper-derived bioactive ceramic, complex-shape implants

1. Introduction

Development of materials for the reconstruction and/or replacement of damaged bones is a one the challenging tasks of biomaterials engineering. A variety of materials and techniques of additive manufacturing have been used to produce a broad range of structures for biomedical applications. Tricalcium phosphate (β-TCP) is a bioresorbable synthetic bioceramic whose chemical composition is close to that of the mineral phase of bone tissue. It has been reported that bone ingrowth (osteoconduction) into β-TCP scaffolds leads to bone regeneration in critical-sized defects [1, 2]. BaG is used to fill and restore bone defects due to its bioactivity and bone-cell stimulating action of its dissolution products [3, 4]. Gmeiner et al. recently reviewed different additive manufacturing techniques for the preparation of bioactive glass (BaG) structures such as stereolithographic ceramic manufacturing, selective laser sintering and dispense plotting [5]. 3D-printing technology was used for the development of structures from BaG, as well as for the fabrication of porous scaffolds for bone ingrowth from hydroxyapatite (HAP)–Ca phosphate ceramic closely resembling bone mineral [6, 7].

Preceramic paper processing approach is a novel technique for the fabrication of ceramics for biomedical applications. It is a cost effective technique for the production of complex-shape ceramic components such as orthopedic and maxillofacial implants. The fabrication of preceramic papers usually involves the use of a paper machine. The process can be subdivided into the initial preparation of an aqueous feed suspension that contains an inorganic filler and a cellulosic fiber or wood pulp, followed by the coagulation of the fiber and the filler in the suspension using polymeric additives and, finally, the formation of the paper sheet by dewatering the feedstock in the paper machine [8]. Paper-derived ceramics are obtained by heat treatment of the preceramic papers due to the burn out of the organic fraction. This leads to a porous ceramic structure [9]. The process is used to achieve a wide variety of complex geometric shapes with specific microstructures and macro- and microscopic porosities with a broad field of applications [7, 8, 10, 11].

The pulp fibers are made of wood plants such as pine and eucalyptus. They are about 1–4 mm long and around 10–30 μm thick. Various inorganic fillers can be used to obtain different structures for specific applications, like alumina and MAX-phases for light-weight structures [12]. In addition to the fibers and the filler, organic additives are used during paper processing. Depending on the type and amount of filler, the amount of anionic and cationic starch and other retention aids like latex have to be chosen. Dried preceramic papers can be processed by several routes in

* *Corresponding author*
Prof. Nahum Travitzky

Table 1. Properties of filler specimens

Specimen	Particle size, μm	Density, g/cm³
β-TCP	3	3.14
HAP	4	3.15
BaG	7	2.73

Table 2. Feedstock composition for preceramic paper processing

Specimen	Pulp fibers, vol %	Filler, vol %	Starch, vol %
β-TCP	26–46	50–70	4
HAP	22–42	50–70	8
BaG	31–41	55–65	4

order to achieve the desired mechanical properties. Calendering influences the density of the preceramic paper and, thereby, of the paper-derived ceramics. Schlordt et al. showed that for preceramic papers containing Al_2O_3 filler the density was increased by 60% before sintering and by 20% for the sintered ceramics [13]. Paper-derived ceramics have a very high open porosity. By coating the preceramic papers with e.g. silica suspension or preceramic polymers, the open porosity can be reduced from around 24% to around 3% for paper-derived alumina. This leads to an increase of the mechanical strength of the sintered ceramics from ~300 to ~350 MPa [14].

For producing paper models of complex shapes, laminated objective manufacturing (LOM) is one of the most widely used techniques. Three-dimensional objects are generated by sequential stacking, laminating, and shaping of the paper sheets. Each layer is cut by a special tool, usually by laser cutting. The paper sheets are then bonded to the previous layer with a thermoplastic adhesive coating on the bottom side of the paper sheet, which may be easily achieved by spraying or screen printing. The adhesive coating is activated by heat and pressure during the process. Having constructed the part, any remaining excess material is removed which is known as decubing. Improvement of the surface quality and strength usually requires resin infiltration and polishing [7, 8, 10].

This paper compares the properties of preceramic papers and paper-derived ceramics for medical applications with different bioactive ceramic fillers: β-TCP, HAP and BaG. Paper processing, sintering behavior and microstructure were analyzed. In order to increase the density and hence reduce porosity in the sintered ceramic product, the effect of pressure application prior to sintering was investigated. LOM was used to fabricate complex structures from the bioactive ceramic filler based preceramic papers.

2. Paper processing

The chemical composition of the used bioactive glass (BaG) was 13–93 was 6 wt % Na_2O, 12 wt % K_2O, 5 wt % MgO, 20 wt % CaO, 4 wt % P_2O_5 and 53 wt % SiO_2. The grain size and density of the fillers are given in Table 1. Table 2 shows the composition of the feedstock for preparation of preceramic papers. The aqueous suspension of a pulp mixture containing 0.30 wt % non-refined softwood pulp with an average diameter of 15 μm and an average length of 657 μm (Celbi PP, Celulose Beira Industrial (Celbi) S.A, Figueira da Foz, Portugal) was homogenized by vigorous stirring at pH = 7.6 for 1 h. The bioactive ceramic filler was added to the aqueous pulp suspension. Solid retention was obtained by flocculation in the feedstock suspension, induced by addition of cationic starch ether (Fibraffin K72, Südstärke GmbH, Schrobenhausen, Germany) and anionic starch ester (Fibraffin A5, Südstärke GmbH, Schrobenhausen, Germany). Both cationic starch ether and anionic starch ester were applied as 1 wt % colloidal aqueous solutions. The preceramic paper sheets were then processed by the Rapid Köthen process on a paper sheet forming device. Circular sheets with a diameter of 200 mm were obtained after dewatering under vacuum ($<10^4$ Pa). The specimens were then dried at 93°C for 15 min resulting in preceramic paper sheets. Preconsolidation of preceramic papers filled with HAP, β-TCP and BaG was done by calendering with a maximum load of 40 N/mm at a temperature of 70°C and a speed of 0.5 mm/min. The preceramic papers were sintered at different temperatures and various dwell times. Specimens with the β-TCP and HAP fillers were sintered at 1200°C, 2 h and 1250°C, 1 h, respectively, and specimens with BaG filler were sintered at 630°C for 1 h. The apparent density of the preceramic paper sheets was determined from the weight and volume measurements. The porosity of the specimens was determined by the Archimedes method (EN 623-2:1993, Germany), using distilled water. The chemical phase analysis of sintered and post-polished samples was evaluated by Energy-dispersive X-ray spectroscopy (EDX, INCA x-sight TVA3, Oxford Instruments, Oxford, UK). The microstructure was examined by scanning electron microscopy (SEM, Quanta 200, FEI, Prag, Czech Republic). The strength of the sintered ceramic specimens was measured using the ball on three ball test (Instron 5565, Instron Corp., Canton, MA, USA) with a constant

Table 3. Composition of the adhesive for LOM processing of HAP-filled preceramic paper

	Wet, wt %	Dry, wt %	Dry, vol %
Planatol AD95	40.42	46.80	70
HAP filler	42.90	49.67	25
Dispersant	3.05	3.53	5
Water	13.62	–	–

crosshead speed of 0.5 mm/min. Young's modulus was derived from the load-displacement curves obtained from 3-point-bar-bending experiments applying a constant crosshead velocity of 0.5 mm/min. The investigation of the density, porosity, shrinkage as well as of bending strength and Young's modulus is described in more detail by Stares et al. [15–17].

Laminated object manufacturing was used to generate three-dimensional ceramic bodies by sequel stacking, laminating, and shaping of the preceramic paper sheets. The preceramic paper sheets were coated with a thermoplastic adhesive (Planatol AD95, Planatol Holding GmbH, Rohrdorf, Germany). The composition of the adhesive with HAP filler is shown in Table 3. Preforms of the preceramic paper sheets were produced by a LOM device (Helisys 1015plus, Helisys Inc, USA) equipped with a heated lamination roller and a laser cutting system. The laser cutting system included a 25 W continuous wave (cw) CO_2 laser operating at a wavelength of 10.6 μm. Lamination was carried out at 140°C using the forward and reverse heater speeds of 40 mm·s^{-1}. The working platform was retracted by 0.1 mm to ensure layer bonding during lamination. The structures consisted of 10 layers with a thickness of 410 μm.

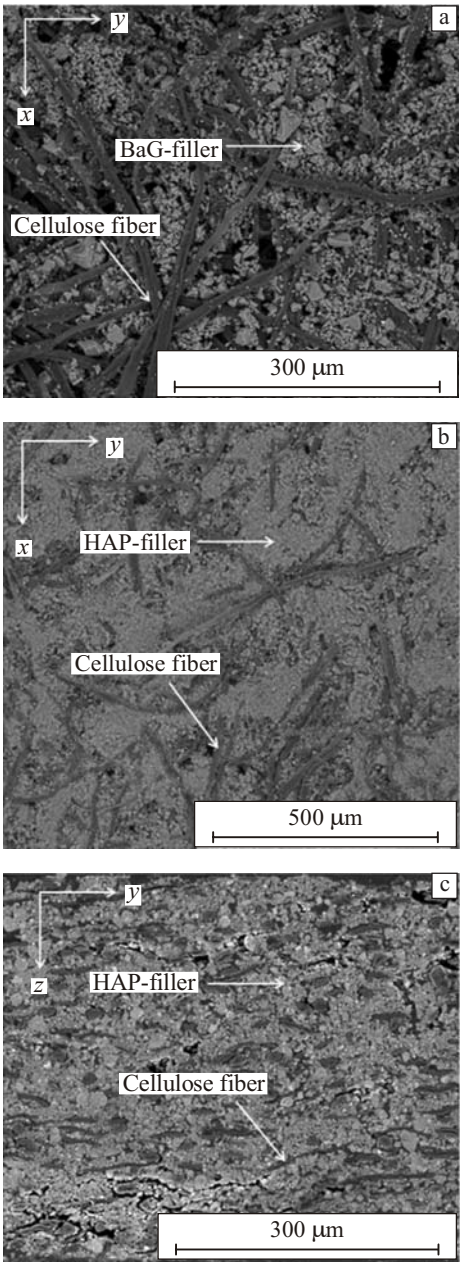

Fig. 1. SEM micrographs of preceramic paper loaded with 60 vol % bioactive ceramic filler: BaG-filler, top surface view (a); HAP-filler, top surface view (b); HAP-filler, cross-sectional view (c).

Table 4. Properties of preceramic papers

Specimen	Open porosity, vol %	Thickness, μm	Density, g/cm³
β-TCP	63–65	1053–1247	0.83–0.95
HAP	72–75	403–410	0.60–0.67
BaG	66–67	257–288	0.72–0.76

3. Properties of preceramic papers and paper-derived biomaterials

Previous works have shown that the properties of as-fabricated paper such as thickness, porosity, density, and

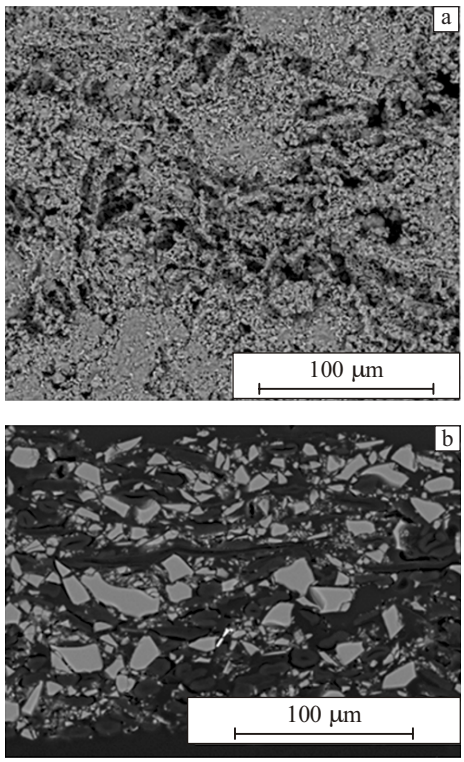

Fig. 2. Sintered paper-derived specimens: HAP (a); BaG (b).

Table 5. Properties of paper-derived specimens

Specimen	Open porosity, vol %	Density, g/cm³	Shrinkage *x*–*y*-direction, %	Shrinkage *z*-direction, %
β-TCP	58–64	1.13–1.31	57–60	2–4
HAP	51–56	0.94–1.37	27–33	2–6
BaG	37–47	1.31–1.67	51–56	3–5

tensile strength were strongly dependent on the fibers and fillers content [15–17]. Table 4 shows the properties of the preceramic papers with different filler types. The open porosity ranges from 63 to 75 vol %. For all specimens, paper density increases with increasing filler content at constant volume, which can be attributed to the higher density of the filler (2.73 to 3.15 g/cm³) compared to the density of the fibers (1.58 g/cm³) [18]. Likewise, the distribution of the fillers in the fiber network depends on filler properties, the fiber network and papermaking conditions. However, with an increase in the filler content, the fiber network expands, resulting in an increased thickness and therefore an increased porosity [19]. Calendering at a load of 40 N/mm of papers filled with BaG leads to an increase of density from 0.72–0.76 g/cm³ to 0.92–0.96 g/cm³, and to decrease of porosity from 66–67% to 56–58% depending on the filler content. Preconsolidation with BaG filled papers was also performed by uniaxial pressing. By applying a maximum pressure of 40 MPa the porosity was decreased from 66–67% to 61–62% and the density was increased from 0.72–0.76 g/cm³ to 0.86–0.87 g/cm³.

Figure 1 shows representative images of the microstructure of the HAP-loaded and BaG-loaded preceramic paper after the sheet-forming process. The ceramic fillers are homogeneously distributed between the cellulose fibers. The fibers are highly oriented perpendicular to the *z* direction compared to a low degree of preferential orientation in the *x*–*y* plane. The characterization of the spatial variation of density, which corresponds directly to the filler distribution in the paper sheets, is very important to control the shrinkage during sintering. By controlling the shrinkage, build-up of residual stress and therefore delamination during processing of multilayer ceramics, can be avoided [8].

The heat treatment of the preceramic papers leads to a significant shrinkage of the as-fabricated specimen. The shrinkage in *z*-direction is in the range of 2 to 6% for all specimens. In the *x*- and *y*-direction, the shrinkage is much higher. For the paper with HAP filler, the shrinkage of 27 to 33% was observed, whereas for the other two materials the shrinkage in the x- and y-directions was in the range of 51 to 60%. The anisotropic shrinkage behavior is associated with the spatial variation of powder packing density, the orientation of the pore/solid interface, the alignment of anisotropic particles, and the introduction of joining and bonding interfaces in multilayer packages [20–22]. The densities of the sintered specimens ranged from 0.94 to 1.67 g/cm³. With increasing filler content, the packing density of the paper-derived specimens was increased, but in the sintered products higher porosity was observed. Nevertheless the porosity of thr sintered specimens is still in the range of 37 to 64 vol %. During sintering the cellulose fibers decompose, leaving behind pores with a morphology and distribution given by the pulp fibers template [8]. The pores could not be closed during sintering and therefore a high open porosity in the sintered specimens remains, which is shown in Fig. 2. The values for the discussed properties are shown in Table 5.

It was shown that the properties strongly depend on preconsolidation of the preceramic papers. By calendering the density of the specimens was highly increased and the vo-

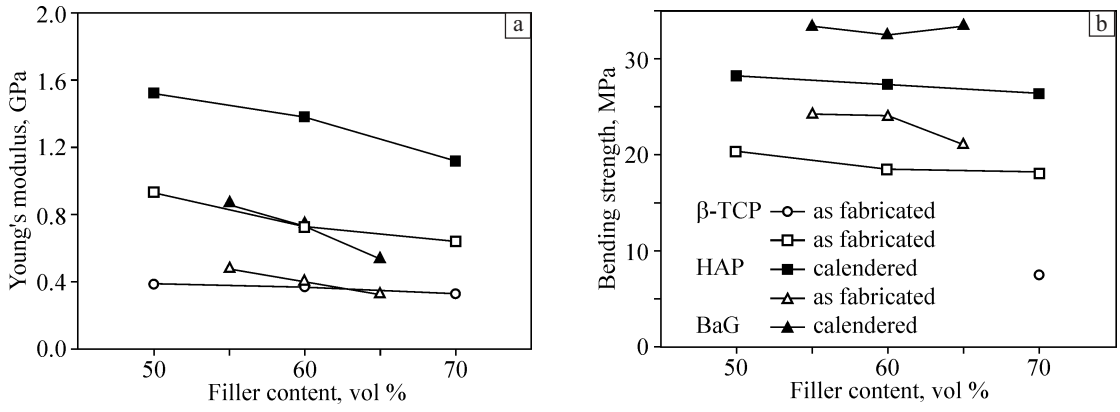

Fig. 3. Bending strength and Young's modulus of paper-derived biomaterials.

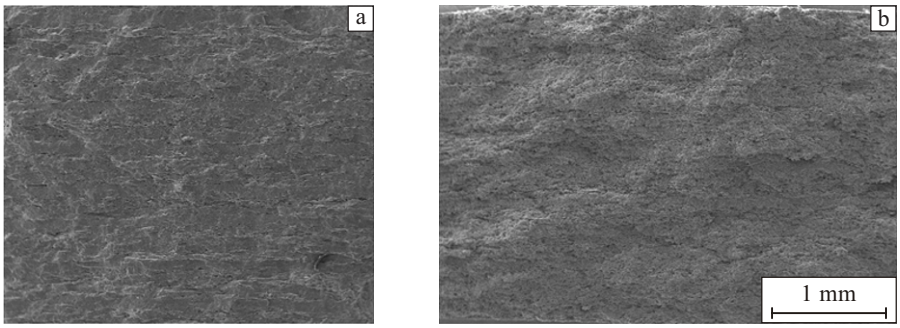

Fig. 4. Fracture surface of HAP (a) and β-TCP (b) samples.

lume fraction of open porosity reduced [15–17]. The apparent densities of the sintered HAP specimens were 0.94–1.37 g/cm³ (as-fabricated) and 1.30–1.59 g/cm³ (pre-consolidated) and the open porosities were 51–56 % and 42–57%, respectively. The apparent densities of sintered BaG specimens were 1.31–1.67 g/cm³ (as-fabricated) and 1.49–1.89 g/cm³ (pre-consolidated) and the open porosity achieved 37–47% and 26–41%, respectively. The apparent densities of the sintered β-TCP specimens were 1.13–1.31 g/cm³ (as-fabricated) and 1.29–1.71 g/cm³ (pre-consolidated) and the open porosities were 58–64% and 42–46%, respectively.

Figure 3 shows the bending strength of the paper-derived specimens. The values for all as-fabricated paper-derived specimens range from ~7.6 to ~24.2 MPa. By calendering, the mechanical strength was increased from ~20 to ~28 MPa for specimens prepared from the paper with HAP filler and from ~24.2 to ~33.1 MPa for specimens prepared from the paper with BaG filler. In all the specimens, the bending strength increased with decreasing volume fraction of open porosity. A 10% increase of porosity leads to a decrease of the strength of sintered ceramics by half of their initial respective values [23]. This leads to the low bending strength of the prepared specimens with β-TCP filler as compared to those with BaG and HAP fillers. A decrease of porosity in the specimens also results in an increased Young's modulus. According to Fig. 3 showing all the specimens with various filler contents after various processing routes, the Young's modulus can be varied in the range of 0.33 to 1.53 GPa. The presented mechanical properties are in the range of the strength (7.6 to 20.7 MPa) and Young's modulus (0.05 to 0.5 GPa) of trabecular bone [24, 25]. Therefore, the presented paper-derived biomaterials show a high potential for the bone replacement applications [26]. Figure 4 shows the fracture surface of the HAP and β-TCP based specimens.

In Fig. 5 X-ray diffraction patterns of the sintered specimens are shown. As expected, the BaG samples are amorphous after sintering. The main phases in the shown β-TCP and HAP curves are $Ca_3(PO_4)_2$ and $Ca_5(PO_4)_3(OH)$, respectively. Despite the burnout of cellulose fibers and the high temperature of 1250°C, the HAP filler material remained stable during sintering. In good agreement with literature, the sintered specimens do not decompose during heat treatment [27, 28].

By using the LOM technique, laminated structures as well as complex shape structures based on preceramic papers can be fabricated. Figure 6 shows HAP and β-TCP samples with cylindrical holes in laminated structures. The microstructure of these specimens is shown in Fig. 7. In addition to LOM technique, highly porous ceramic structures can be prepared by perforation of preceramic papers before sintering. As a proof of concept, perforated HAP specimens with holes in the range from 150 μm to around 500 μm required for bone ingrowth, were fabricated (Fig. 8).

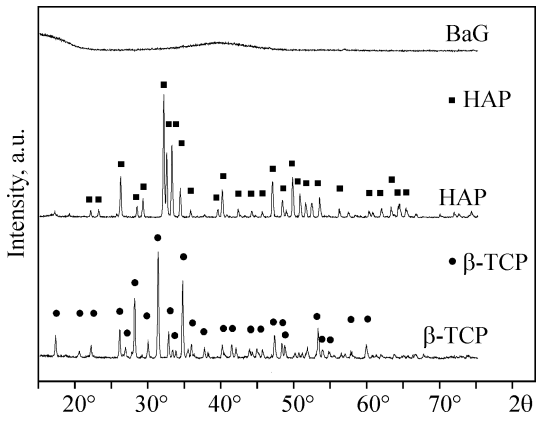

Fig. 5. Diffraction scan of samples after sintering.

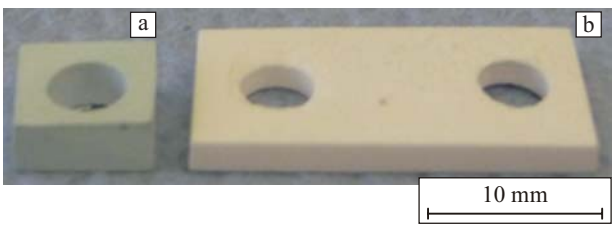

Fig. 6. Complex shape geometries of HAP (a) and β-TCP (b) samples after sintering.

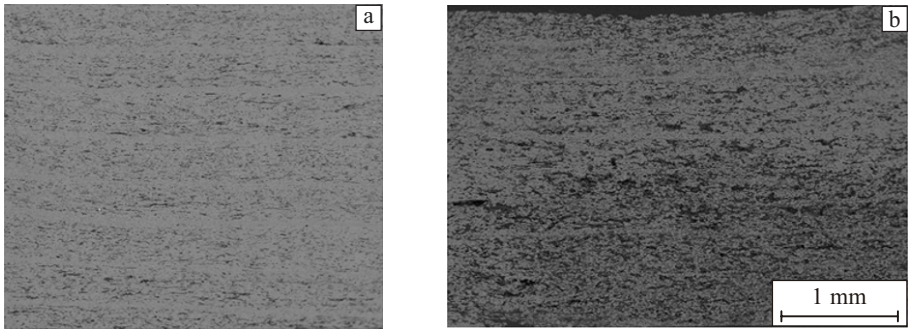

Fig. 7. Microstructure of laminated HAP (s) and β-TCP (b) structures.

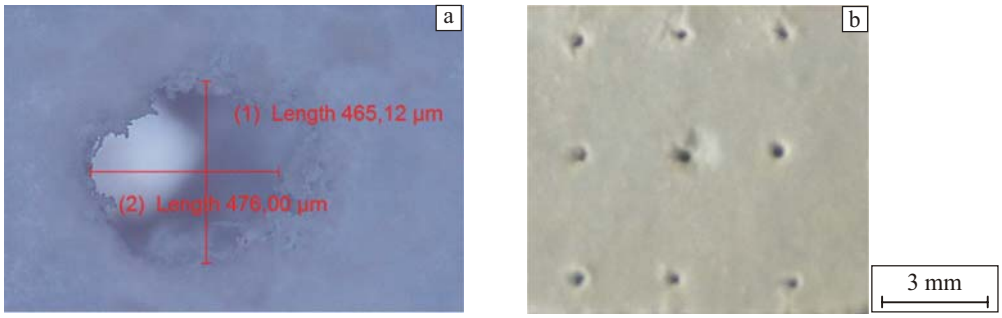

Fig. 8. Perforated HAP specimens.

4. Summary

In the present work, different paper-derived bioactive ceramics—β-TCP, HAP and BaG were fabricated and compared. The preceramic papers were prepared by the Rapid Köthen process with different β-TCP, HAP and BaG fillers for use in bone reconstruction surgery. It was shown that large flat sheets of paper-derived biomaterials can be produced by this process. The properties of the final products were compatible with the necessary requirements for bone replacement applications such as fabricating load-bearing scaffolds to repair trabecular bone defects. It was shown that preceramic paper processing approach can be used for fabrication of complex shape ceramic products for biomedical applications and especially for production of implants for bone replacement.

References

1. Seebach C, Henrich D, Kähling C, Wilhelm K, Tami AE, Alini M, Marzi I. Endothelial progenitor cells and mesenchymal stem cells seeded onto â-TCP granules enhance early vascularization and bone healing in a critical-sized bone defect in rats. Tissue Eng A. 2010; 16: 1961–1970.
2. Xu L, Lv K, Zhang W, Zhang X, Jiang X, Zhang F. The healing of critical-size calvarial bone defects in rat with rhPDGF-BB, BMSCs, and â-TECP scaffolds. J Mater Sci Mater Med. 2012; 23: 1073–1084.
3. Oh S, Oh N, Appleford M, Ong JL. Bioceramics for tissue engineering applications—a review. Am J Biochem Biotech. 2006; 2: 49–56.
4. Bombac D, Brojan M, Fajfar P, Kosel F, Turk R. Review of materials in medical applications. RMZ–Mater Geoenvironment. 2007; 54: 471–499.
5. Gmeiner R, Deisinger U, Schönherr J, Lechner B, Detsch R, Boccaccini AR, Stampfl J. Additive manufacturing of bioactive glasses and silicate bioceramics. J Ceram. Sci. Tech. 2015; 06: 75–86.
6. Will J, Melcher R, Treul C, Travitzky N, Kneser U, Polykandriotis E, Horch R, Greil P. Porous ceramic bone scaffolds for vascularized bone tissue regeneration. J Mater Sci Mater Med. 2008; 19: 2781–2790.
7. Travitzky N, Bonet A, Dermeik B, Fey T, Filbert-Demut I, Schlier L, Schlordt T, Greil P. Additive manufacturing of ceramic-based materials. Adv Eng Mater. 2014; 16: 729–754.
8. Travitzky N, Windsheimer H, Fey T, Greil P. Preceramic paper-derived ceramics. J Am Ceram Soc. 2008; 91: 3477–3492.
9. Dasgupta S, Das SK. Paper pulp waste—a new source of raw material for the synthesis of a porous ceramic composite. Bull Mater Sci. 2002; 25: 381–385.
10. Windsheimer H, Travitzky N, Hofenauer A, Greil P. Laminated objective manufacturing of preceramic-paper-derived Si-SiC composites. Adv Mater. 2007; 19: 4515–4519.
11. Gutbrod B, Haas D, Travitzky N, Greil P. Preceramic paper derived alumina/zirconia ceramics. Adv Eng Mater. 2011; 13: 494–501.
12. Schultheiß J, Dermeik B, Filbert-Demut I, Hock N, Yin X, Greil P, Travitzky N. Processing and characterization of paper-derived Ti_3SiC_2 based ceramic. Ceram Int. 2015; 41: 12595–12603.
13. Schlordt T, Dermeik B, Beil V, Freihart M, Hofenauer A, Travitzky N, Greil P. Influence of calendering on the properties

of paper-derived alumina ceramics. Ceram Int. 2014; 40: 4917–4926.
14. Junkes JA, Dermeik B, Gutbrod B, Hotza D, Greil P, Travitzky N. Influence of coatings on microstructure and mechanical properties of perceramic paper-derived porous alumina substrates. J Mater Process Tech. 2013; 213: 308–313.
15. Stares SL, Fredel MC, Greil P, Travitzky N. Paper-derived hydroxyapatite. Ceram Int. 2013; 39: 7179–7183.
16. Stares SL, Fredel MC, Greil P, Travitzky N. Paper-derived â-TCP. Mater Lett. 2013; 98: 161–163.
17. Stares SL, Kirilenko A, Fredel MC, Greil P, Wondraczek L, Travitzky N. Paper-derived bioactive glass tape. Adv Eng Mater. 2013; 15: 230–237.
18. Niskanen K. Papermaking science and technology: Paper physics. in: Finnish paper engineerss' association. 2nd ed. Helsinki: Paperi Ja Puu Oy; 2008: 20–26.
19. Bown R. The effect of particle size and shape of paper fillers on paper properties. Wochenbl Papierfabr. 1983; 111: 737–740.
20. Exner HA, Geiss EA. Anisotropic shrinkage of cordierite-type glass powder cylindrical compacts. J Mater Res. 1988; 3: 122–125.
21. Raj PM, Cannon WR. Anisotropic shrinkage in tape-cast alumina: Role of processing parameters and particle shape. J Am Ceram Soc. 1999; 82: 2619–2625.
22. Lin YC, Jean JH. Constrained densification kinetics of alumina/borosilicate glass + alumina/alumina sandwich structure. J Am Ceram Soc. 2002; 85: 150–154.
23. Ryshkewitch E. Compression strength of porous sintered alumina and zirconia. J Am Ceram Soc. 1953; 36: 65–68.
24. Stone JL, Beaupre GS, Hayes WC. Multiaxial strength characteristics of trabecular bone. J Biomech. 1983; 16: 743–747, 749–752.
25. Kaplan SJ, Hayes WC, Stone JL, Beaupré GS. Tensile strength of bovine trabecular bone. J Biomech. 1985; 18: 723–727.
26. Kolan KCR, Leu MC, Hilmas GE, Brown RF, Velez M. Fabrication of 13-93 bioactive glass scaffolds for bone tissue engineering using indirect selective laser sintering. Biofabrication. 2011; 3: 025004.
27. Cihlar J, Buchal A, Trunec M. Kinetics of thermal decomposition of hydroxyapatite bioceramics. J Mater Sci. 1999; 34: 6121–6131.
28. Rapacz-Kmita A, Paluszkiewicz C, Slosarczyk A, Paszkiewicz Z, FTIR and XRD invesigations on the thermal stability of hydroxyapatite during hot pressing and pressureless sintering process. J Molecular Sci. 2005; 744–747: 653–656.